Synthesis of 4-Chloro-3-nitrobenzotrifluoride: Industrial thermal runaway simulation due to cooling system failure

Sabrina Copelli[a], *Marco Derudi*[b], *Carlo Sala Cattaneo*[b], *Giuseppe Nano*[b], *Massimo Raboni*[a], *Vincenzo Torretta*[a], *Renato Rota*[b,*]

[a] *Università degli Studi dell'Insubria, Dipartimento di Scienza e Alta Tecnologia, via G.B. Vico, 46, 21100 Varese, Italy*

[b] *Politecnico di Milano, Dipartimento di Chimica, Materiali e Ingegneria Chimica "G. Natta", via Mancinelli, 7, 20131 Milano, Italy*

1. Introduction

Runaway phenomena in chemical reactors have been thoroughly analyzed in the process safety literature of the last twenty five years (e.g., Steensma and Westerterp, 1988; Balakotaiah et al., 1995; Alós et al., 1998; van Woezik and Westerterp, 2000; Zaldívar et al., 2003; Bosch et al., 2004; Varma et al., 2005; Mas et al., 2006; Maestri et al., 2009a; Copelli et al., 2011a,b; Jiang et al., 2011; Maria and Stefan, 2011; Casson et al., 2012), even performing full-scale experimental tests (Linga et al., 2013). It is well known that a runaway reaction is the consequence of a reacting system thermal loss of control that can be triggered by a number of upset operating conditions: e.g., pumps failure, cooling system breakdown, temperature controller anomalies or external fire. This situation, also called thermal explosion, is responsible for an increase of the desired reaction rate and can also lead to the triggering of unwanted decomposition reactions of the reacting mixture with consequent reactor pressurization due to incoercible gases formation. Moreover, if the internal reactor pressure overcomes a critical value (P_{cr}), the reactor can explode releasing high amounts of toxic and/or flammable gases into the atmosphere and leading to disastrous consequences for both the workers and the inhabitants of the damaged factory neighboring. Terrible examples of such scenarios are Seveso in 1976, and Bhopal in 1984, accidents. Minor and recent examples are the T2 laboratories accident occurred in Jacksonville, Florida (2007), where 4 workers died

* *Corresponding author*. Tel.: +39 0223993154; fax: +39 02 23993180.
E-mail address: renato.rota@polimi.it (R. Rota).
Received 20 April 2013; Received in revised form 12 November 2013; Accepted 18 November 2013
Available online 1 December 2013

Nomenclature

A	species A (dosed reactant = 4-Cl-BTF); total heat exchanging area, m^2; pre-exponential factor (m^3 s/kmol)
ARC	Accelerating Rate Calorimeter
B	species B (initially loaded reactant = NO_2^+)
C	species C (desired product = 4-Cl-3nitroBTF)
$\hat{c}_p$	mass specific heat (J/(kg K))
D	species D (side product = H_2O)
Da_{dec}	$= (A_{dec} \cdot \exp(-E_{att,dec}/RT_{rif}) \cdot \hat{\rho}_C \cdot t_{rif})/PM_C$, Damkoler number for the decomposition reaction (ARC test)
Da	$A_{1/2} \cdot \exp(-E_{att,1/2}/RT_{rif}) \cdot [B]_0 \cdot t_{dos}$, Damkoler number (reactor synthesis)
E_{att}	activation energy (J/kmol or J/kmol)
f_{dec}	$=(1-\zeta)$, concentration function for the decomposition reaction
f_1	$= [(v_{dos} - \zeta_1)/((\varepsilon./\rho_{dos}) \cdot v_{dos})] \cdot (1-\zeta_1)$, concentration function for reaction (1)
f_2	$= (\zeta_1 - \zeta_2)/((\varepsilon/\rho_{dos}) \cdot v_{dos})$, concentration function for reaction (2)
G	pseudo-species representing all gases evolved during the decomposition reaction
h	total molar enthalpy (J/kmol)
k	kinetic constant (s^{-1} or m^3 s/kmol)
K	constant for static gain and reset time (s^{-1} or m^3 s/kmol)
m	reacting mass (kg)
MAT	Maximum Allowable Temperature (°C)
$MTSR$	Maximum Temperature due to Synthesis Reaction (°C)
n	number of moles (kmol)
NTU	Number of Transport Unit
p	$=P/P_{rif}$, dimensionless pressure
P	pressure (atm or psia)
r	reaction rate (kmol/(m^3 s))
R	ideal gas constant = 8314 J/(kmol K)
RE_1	Reactivity Enhancement factor for reaction (1)
R_H	heat capacity ratio
St	$= (UA)_{0/ext} \cdot t_{dos}/(\hat{\rho}_0 \cdot \hat{c}_{p,mix} \cdot V_0)$, Stanton number
T	temperature (°C or K)
t	time (s or min)
U	overall heat transfer coefficient (W/(m^2 K))
v	$=V/V_0$, dimensionless total liquid volume
V	total liquid volume (m^3)
$\dot{V}$	volumetric flow rate (m^3/s)

Subscripts and superscripts

ad	adiabatic temperature rise
air	gas in the reactor headspace
att	activation energy
$cool$	jacket/coolant
cr	critical value
dos	dosing period
eb	boiling point
ext	external environmental conditions
g	gaseous/vapor phase
H	heat capacity ratio
$hold$	sample holder for the ARC HWS test
i	ith species (C or G)
IN	inlet stream
iT	reset time of the temperature controller (s)
j	jth reaction (1) or (2)
l	liquid phase
mix	reacting mixture loaded into the ARC sample holder
nom	nominal volume of the reactor
p	process
pT	proportional gain of the temperature controller
rif	reference conditions
rxn	reaction
set	set-point value
top	top part of the reactor (that one filled with inert gases)
TOT	total amount
0	start of the dosing period
1	first reaction (desired reaction)
2	second reaction (decomposition reaction)

Greek symbols

γ	$=E_{att}/RT_{rif}$, dimensionless activation energy
$\Delta\tilde{H}$	reaction enthalpy (cal/kmol or J/kmol)
ε	$= m_{dos,TOT}/m_0$, mass ratio
ζ	conversion with respect to the desired product
κ	$= \exp(\gamma(1-1/\tau))$, dimensionless kinetic constant
ϑ	$=t/t_{dos}$, dimensionless time
θ	$= V \cdot t_{dos}/\dot{V}$, dimensionless residence time
ρ	$\hat{\rho}/\hat{\rho}_0$, dimensionless total liquid density
$\hat{\rho}$	total liquid density (kg/m^3)
τ	$=T/T_{rif}$, dimensionless temperature
Φ	$= (m_{mix} \cdot \hat{c}_{p,mix} + m_{hold} \cdot \hat{c}_{p,hold})/(m_{mix} \cdot \hat{c}_{p,mix})$, thermal inertia factor

and 32 people were injured, and the Bayer CropScience LP one, occurred in West Virginia (2008), where 2 workers died and 8 people were injured (CSB, 2013).

Historically, in order to evaluate the consequences of a runaway, the main data required are: rate of heat evolution due to chemical reactions taking place into the system and reactor cooling efficiency. Particularly, it is necessary to know reaction enthalpy and heat capacity of the reacting mixture, adiabatic temperature rise under process conditions, boiling point of the reacting mixture (if any), temperature range in which dangerous decomposition reactions can be triggered and their reaction enthalpy, amount and rate of gas evolution, effect of operational errors and impurities. Through a combination of these process information, Stoessel (1993, 2009) classified exothermic reaction processes into five classes as a function of the relative ranking of: process temperature (T_p), maximum temperature that can be achieved by synthesis reaction as a consequence of cooling system failure ("Maximum Temperature due to Synthesis Reaction", *MTSR*), boiling point of the solvent (T_{eb}), Maximum Allowable Temperature (*MAT*) to avoid decomposition reactions taking place. Situations characterized by *MTSR* values higher than the *MAT* values must be regarded as critical from a safety point of view: for instance, a less exothermic reaction system with a relatively low decomposition temperature can be much more dangerous than a more exothermic one with a very high decomposition temperature.

Such a thermal classification is very useful for a quick and easy evaluation of the hazard associated with a process operated in runaway conditions, such as that associated to a cooling system failure (which is one of the main causes of runaway reactions triggering in full scale plant). However, since it summarizes all data related to unwanted side reactions into a single pieces of information, the *MAT* parameter, it does not permit to evaluate in details the runaway consequences arising from different accidental scenarios.

Several literature studies have investigated reactor safety with a specific attention to the problem of a loss of coolant or a failure of the cooling system (Balchan et al., 1999; Kossoy and Akhmetshin, 2012; Luyben, 2012). Balchan et al. (1999) realized a dynamic model to simulate the runaway behavior of a radical solution polymerization reactor; the model was validated with a self-heating rate profile of the reacting mixture obtained in few calorimetric experiments and it was used to evaluate the sizing procedure of reactor emergency reliefs. Kossoy and Akhmetshin (2012) developed a stability analysis model, based on a non-linear optimization method, to perform a safety analysis of the esterification reaction between propionic anhydride and isopropyl alcohol, while Luyben (2012) used Aspen Dynamics to predict different accidental scenarios that can occur in typical CSTR and tubular chemical reactors. Some of these studies were based on a simplified description of the investigated processes and none of the proposed models was validated with experimental data related to overpressure profile obtained under runaway conditions.

In order to ensure a full description of runaway phenomena and related overpressure buildup problems at full plant scale, it is very important to take into account all features related to reactants feeding procedures (linear, ramp, etc.), reactor temperature control (isothermal, isoperibolic, etc.) and thermo-chemical stability of the reacting mixture. Therefore, it is necessary to write a suitable system of ordinary differential equations (ODEs) where mixing rules for volumes determination, global and components material balance equations, reactor and jacket energy balance equations, dosing strategies and reactor temperature control equations must be inserted to describe completely the analyzed process dynamics under both normal and upset conditions.

In this work, a dedicated model has been developed, validated and used to simulate a cooling system failure in an industrial isoperibolic SBR ($9\,m^3$) where the nitration of 4-Chlorobenzotrifluoride (4-Cl BTF) to 4-Chloro-3nitrobenzotrifluoride (4-Cl-3nitroBTF – a chemical intermediate) by the means of mixed acids is carried out. Its implementation has been realized using GUIDE, the MATLAB Graphical User Interface Development Environment, which provides a set of tools for creating graphical user interfaces (GUIs) and allows for benefiting all the MATLAB calculation power. The mathematical model on which the software is based is able to simulate both reactor temperature and pressure vs. time profiles, before and during the cooling system breakdown, thanks to a complete description of both the desired reaction (nitration) and the unwanted reacting mixture decomposition kinetics. To manage the software and perform a simulation, only a few experimental parameters are needed; essentially: heats of reaction, apparent system kinetics (Arrhenius law), heat transfer coefficients and reactants heat capacities. For this study, such parameters have been obtained both from literature and Accelerating Rate Calorimeter (ARC) experiments.

2. Mathematical model

On the following, all the equations necessary for the complete system description (implemented into the dedicated accidents simulation software) will be briefly summarized.

Particularly, the desired nitration reaction is assumed to occur as follows:

$$A_{(l)} + B_{(l)} \Rightarrow C_{(l)} + D_{(l)} \tag{1}$$

where *A* and *B* are, respectively, the dosed and loaded reactants, respectively, *C* is the desired product and *D* represents all the side products. In addition to (1), the decomposition reaction of the desired product (formally, species *C*) must be also considered; this reaction is assumed to take place producing a gaseous (*g*) species *G* (*G* is a pseudo-species representing, in real conditions, a mixture of different gases):

$$C_{(l)} \Rightarrow G_{(g)} \tag{2}$$

Reactions (1) and (2) are characterized by their corresponding microkinetic expressions:

$$r_1 = A_1 \cdot \exp\left(-\frac{E_{att,1}}{RT}\right) \cdot [A] \cdot [B] \tag{3}$$

$$r_2 = A_2 \cdot \exp\left(-\frac{E_{att,2}}{RT}\right) \cdot [C]^2 \tag{4}$$

Despite the fact that nitration reactions are among the first processes to be operated on a large scale when heavy organic chemical industry developed at the beginning of the 19th century, many questions about aromatic nitration in mixed acids remain without exhaustive answers. The dynamic behavior of an aromatic nitration in mixed acids involves a number of problems related to simultaneous interphase and intraphase mass transfer phenomena, especially if the synthesis is carried out with reactants in stoichiometric quantities. These phenomena lead to complex problems during characterization and scale-up of such processes, mainly arising from the interdependence among fluid properties (e.g., viscosities, densities, interfacial surface properties, diffusion coefficients, and distribution coefficients among the phases), operating conditions (temperatures) and equipment characteristics (e.g., impeller kind and size, reactor geometry).

Since for the system investigated in this work one of the inorganic acids (namely, the sulfuric one) is in large excess and it acts also as a solvent, the first problem can be avoided by feeding the reactor with mixed acids as initial reactant. The second one strongly influences heat and mass transfer efficiencies, so in order to operate under kinetically controlled conditions (where no heat or mass transfer limitations lower the overall conversion of the process), it is necessary to work with a sufficiently high stirrer speed. Above a certain speed value, no more heat and mass transfer limitations on heat reactor flux are observed. In such conditions, a perfectly macromixed reaction mass is formed, no phase separation effects occur and the characteristic time of mass and heat transfer phenomena is much lower than that one characteristic of the reaction. However, aromatic nitrations develop high heat of reaction and are often accompanied by unwanted reactions that in the past have produced a considerable number of accidents. Therefore, a deep understanding of this kind of problem is very important to safely operate nitration plants.

For the present case-study, the species to be nitrated (that is, 4-Cl BTF) is added to a mixture of sulfuric and nitric acids in which sulfuric acid acts both as a solvent and as a dehydrating agent versus nitric acid to form the nitronium ion, NO_2^+, which is the electrophilic species reacting with the aromatic ring. The overall reaction (1) takes place in the continuous acid phase; with no transfer limitations, the reaction rate of (1) equals the overall conversion rate of the aromatic species to the nitrocompound (limiting step). In this work, the system analyzed has been considered as a heterogeneous (liquid–liquid) system operating in the slow reaction regime, which is known to be the most hazardous one. In such operating conditions, all information related to the desired reaction kinetics can be found in literature (Maestri et al., 2009b; Copelli et al., 2011a). In particular, the microkinetic parameters of reaction (1) are $A_1 = 3.228 \times 10^{12}$ (m^3 s)/kmol and $E_{att,1} = 87{,}260$ kJ/kmol, respectively.

Therefore, the following model assumptions can be reasonably stated:

(1) the reaction mass is perfectly macromixed;
(2) the influence of all chemical reactions on the volume of the liquid phase(s) is negligible;
(3) no phase inversions occur;
(4) the solubility of the species *A* (co-reactant) and *C* in the continuous phase, "c", and of components *B* (reactant initially loaded into the reactor) and *D* in the dispersed phase, "*d*", is small;
(5) the chemical reaction takes place only in one of the two liquid phases: this is very common in many industrial processes (such as nitration and oxidation reactions), in which the catalyst (typically a strong acid) is only in one phase;
(6) heat generation effects are due to the chemical reactions only;
(7) heat removal effects are related to both cooling and ambient dispersions;
(8) the reactor operates under isoperibolic conditions (jacket temperature controlled by a suitable temperature controller);
(9) dosing of species *A* is carried out at a constant rate;
(10) ideal gas behavior.

Considering such hypotheses, the overall system of ordinary differential equations can be written as follows:

$$\begin{cases} \dfrac{dm}{dt} = \varphi_{dos}(t) = \dfrac{m_{TOT,dos}}{t_{dos}} \\ \dfrac{dT_{cool,IN}}{dt} = -K_{pT} \cdot \left[\dfrac{dT_{cool}}{dt} - \dfrac{1}{K_{iT}} \cdot (T_{cool,set} - T_{cool}) \right] \\ \dfrac{dV}{dt} = \varphi_V(t, T, \vec{n}) \\ \hat{\rho}_{cool} \cdot \hat{c}_{p,cool} \cdot V_{cool} \cdot \dfrac{dT_{cool}}{dt} = \hat{\rho}_{cool} \cdot \hat{c}_{p,cool} \cdot \dot{V}_{cool} \cdot (T_{cool,IN} - T_{cool}) + UA \cdot (T - T_{cool}) \\ \dfrac{d(m \cdot h)}{dt} = \dfrac{dm}{dt} \cdot \hat{c}_{p,dos} \cdot (T_{dos} - T_{rif}) + \sum_{j=1}^{2} r_j \cdot (-\Delta\tilde{H}_{rxn,j}) \cdot V_{rxn,j} - UA \cdot (T - T_{cool}) - UA_{ext} \cdot (T - T_{ext}) \\ \dfrac{dn_i}{dt} = \sum_{j=1}^{2} \nu_{i,j} \cdot r_j \cdot V_{rxn,j} \quad i = C, G \\ \dfrac{dP}{dt} \cdot (V_{nom} - V) - P \cdot \dfrac{dV}{dt} = \dfrac{dn_{top}}{dt} \cdot R \cdot T + n_{top} \cdot R \cdot \dfrac{dT}{dt} \end{cases} \quad (5)$$

$$I.C \quad t = 0 \Rightarrow m = m_0, \quad T_{in,cool} = T_{in,cool,0}, \quad V = V_0, \quad T_{cool} = T_{cool,0}, \quad T = T_0, \quad n_i = n_{i,0} \quad P = P_0$$

where m is the total reacting mass (kg), φ_{dos} is the dosing stream function, $T_{cool,IN}$ is the inlet coolant temperature (K), T_{cool} is the actual coolant temperature (K), $T_{cool,set}$ is the set-point temperature of the jacket (K), T is the reactor temperature (K), T_{dos} is the dosing stream temperature (K), T_{ext} is the ambient temperature (K), K_{pT} is the proportional gain of the temperature controller, K_{iT} is the reset time of the temperature controller (s), φ_V is a function accounting for mixing rules (that can assume a number of different time, temperature and compositions dependent expressions), V is the total liquid reacting volume (m^3), h is the molar enthalpy of the reacting mixture (J/kmol), UA is the global heat transfer coefficient for the cooling system (W/K), UA_{ext} is the global heat transfer coefficient for the ambient (W/K), r_j is the jth reaction rate (kmol/(m^3 s)) according to, e.g., Arrhenius Law, $\Delta\tilde{H}_{rxn,j}$ is the jth reaction enthalpy (J/kmol), $\hat{\rho}$ is the density (kg/m^3), and P is the pressure. Other symbols meaning is reported in the Nomenclature section.

Particularly, first and second equations express, respectively, the dosing procedure (in this case, constant feeding rate) and the reactor temperature control mode (in this case, isoperibolic); the third equation synthesizes the mixing rules for density and total volume determination; the following two equations represent the energy balances of the cooling jacket and the reactor, respectively; the sixth equation resumes the material balance of all components and, finally, the seventh equation expresses how the pressure inside the reactor varies, as a function of temperature and the eventual permanent gases formation. The system of Eq. (5) has been made dimensionless to ease its implementation and numerical solution. The resulting system, for the case-study considered in this work, is detailed in Appendix A.

3. Results and discussion

3.1. *Determination of the decomposition reaction kinetics*

In order to study the kinetics of the desired product decomposition, it is necessary to perform a suitable adiabatic test onto the final reacting mixture (that is, the reacting mixture after a normal synthesis operation at low temperatures where no runaway phenomenon has been triggered).

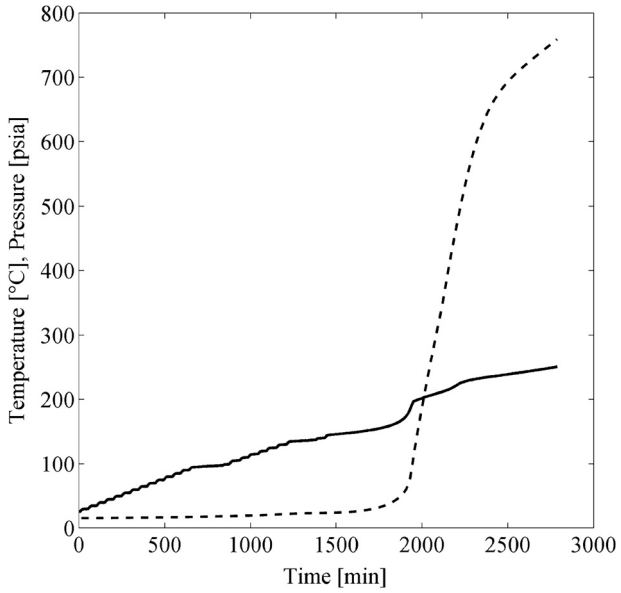

Fig. 1 – ARC thermal characterization of the final reaction mixture (sample amount: 2.55 g; initial temperature: 30 °C, standard "HEAT" – "WAIT" – "SEARCH" test). Legend: (—) Temperature; (- - -) pressure.

The equipment used for this test was an Accelerated Rate Calorimeter (ARC), that is an adiabatic calorimeter particularly suitable to study reacting systems subject to decomposition. It is constituted by a spherical sample holder, built of Hastelloy C and placed in an insulated vessel, a radiant heater which raises sample temperature up to a determined value; moreover, a thermocouple is connected to the sample holder wall in order to record sample temperature while an insulated jacket, with three thermocouples and eight heaters, is used to heat up the oven at the same rate as the one of the sample holder during the exothermic reaction. Finally, a capillary tube allows the connections between the sample holder and a pressure transducer.

A single ARC test allows for obtaining several information, including initial and final temperature of any detected exothermic effect, self-heating rate vs. temperature, adiabatic temperature increase, pressure and pressure increase rate vs. temperature (Shu and Yang, 2002). Results obtained in such experiments can be used with a good degree of reliability even for full plant purposes but they are strictly dependent on the sample holder thermal inertia Φ, which is the ratio between the sum of sample and sample holder heat capacities and the sample heat capacity (Roduit et al., 2008). Consequently, experimental data have to be corrected to take into account this effect before being used at other scales (such as the full plant or the pilot) where Φ factor is normally closed to unity.

In this work, after the desired synthesis has been performed into a 50 mL flask, 2.55 g of the final reacting mixture has been loaded into the ARC sample holder and a standard HWS ("HEAT" – "WAIT" – "SEARCH") test (Pasturenzi et al., 2013) has been started from an initial temperature equal to 30 °C. Temperature and pressure profiles measured in the ARC experiment are shown in Fig. 1.

A strong exothermic effect can be identified at 141 °C, which implies a huge pressure increase due to the decomposition of the reaction mass with the production of permanent gases.

The main parameters estimated from the ARC experiment results are summarized in Table 1. These values have been corrected according to the sample holder thermal inertia, as synthesized by the Φ factor.

Table 1 – ARC test on final reacting mixture: thermo-chemical properties of reaction mass decomposition.

Starting temperature	414 (K)
Starting pressure	1.64 (bar)
Starting self heating rate	0.0064 (K/s)
Final instrumental temperature	528 (K)
Final instrumental pressure	46.87 (bar)
Instrumental adiabatic temperature rise	387 (K)
Calorimeter thermal inertia factor	2.846
Adiabatic temperature rise	325 (K)
Final reaction temperature	739 (K)
Decomposition enthalpy	−438 (kJ/kg)

Table 2 – Pre-exponential factors and activation energies for the final reacting mixture decomposition reaction.

Temperature range (°C)	A_2 ((m^3 s)/kmol)	$E_{att,2}$ (kJ/kmol)
$T \leq 197$	2.718×10^7	108,279
$197 < T \leq 216$	3.814×10^6	108,940
$216 < T \leq 226$	2.783×10^6	107,940
$T > 226$	1.276×10^4	92,121

Using Eq. (4) and both temperature and pressure profiles of Fig. 1, it is possible to determine the reacting mixture decomposition kinetics through a data fitting carried out using model equations reported in Appendix B. The resulting reaction rate parameters are reported in Table 2. A comparison between model results and experimental data is reported in Fig. 2, showing a good agreement.

3.2. *Numerical analysis*

In this section dynamic simulations of both normal and upset (cooling system failure) operating conditions, referring to a 9 m^3 indirectly cooled SBR operated in the isoperibolic temperature control mode, are reported and compared.

3.2.1. *Normal conditions*

Industrial reactor characteristics and normal operating conditions for this process are summarized in Table 3 (Maestri et al., 2009b).

Fig. 3a and b report temperature and desired product conversion vs. time profiles, respectively, while Fig. 3c shows the corresponding pressure vs. time profile during the synthesis.

As it can be noticed, reactor temperature profile is very sharp but the maximum temperature which is reached (107 °C) is much lower than the threshold value of 141 °C (*MAT*) in correspondence of which a strong decomposition of the reacting mixture has been observed into the ARC test. From the analysis of both the desired conversion and pressure profile it is possible to conclude that no decompositions of the reacting mixture occurs at the temperatures reached during the

Table 3 – Characteristics and operating parameters for the industrial reactor.

$(UA)_0$	4910 (W/K)	T_0	308 (K)
$\hat{\rho}_0$	1787 (kg/m^3)	ΔT_{ad}	129 (K)
$\hat{\rho}_{dos}$	1353 (kg/m^3)	t_{dos}	3600 (s)
$\hat{c}_{p,0}$	1.477 (kJ/(kg K))	$[B]_0$	2.764 (kmol/m^3)
$\hat{c}_{p,dos}$	0.869 (kJ/(kg K))	m_A	0.01
V_0	4.688 (m^3)	V_{dos}	1.633 (m^3)

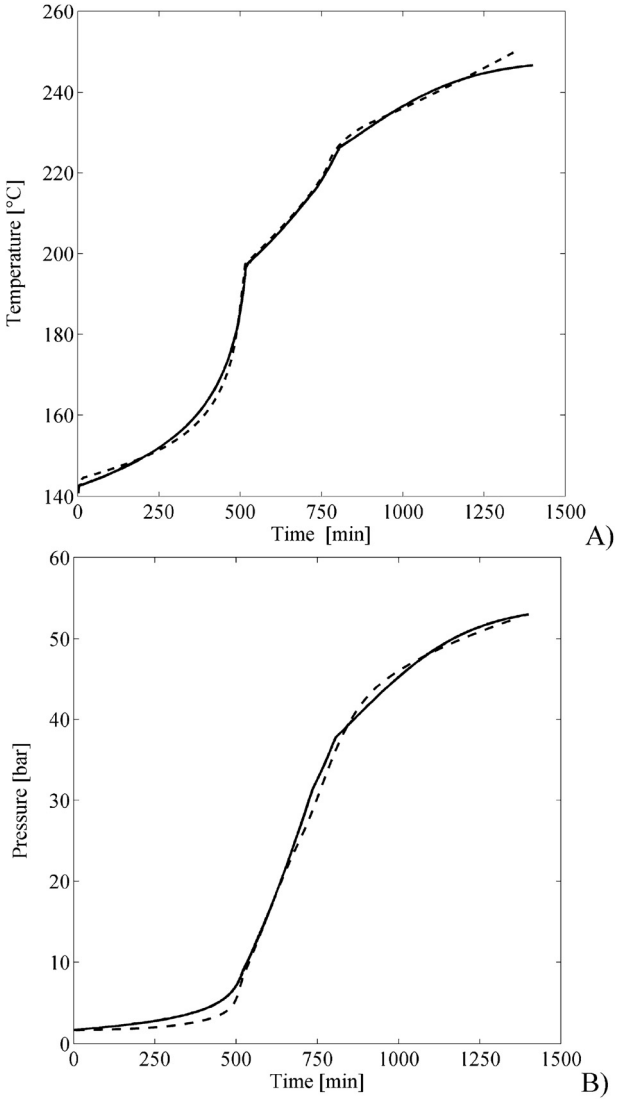

Fig. 2 – Results of the fitting procedure for the decomposition reaction. Comparison between experimental results (- - -) and theoretical predictions (—). (A) Temperature vs. time profiles; (B) pressure vs. time profiles.

synthesis because the maximum conversion is obtained and there is no pressure increase at the end of the synthesis (the only pressure increase is due to the temperature increase during the reaction but it expires rapidly when the temperature goes down as a consequence of the synthesis completion).

3.2.2. *Upset conditions*

One of the most frequent causes of industrial equipment failure is the breakdown or the loss of control of the coolant pumping system (Gygax, 1988; Farquharson et al., 1997; Svandova et al., 2005; Kidama and Hurme, 2013). This accident involves the absence of cooling liquid circulation into the reactor jacket with the consequent establishment of nearly adiabatic operating conditions. With reference to the investigated process, Fig. 4 shows conversion, temperature and pressure profiles referring to a cooling system failure occurring at 1/3, 2/3 and 1.5 of the dosing time period, respectively.

When a cooling system failure occurs during the first part of the dosing period, that is at 1/3 of t_{dos} (continuous lines in Fig. 4), the conversion with respect to the desired product C increases rapidly due to the nitration reaction and, then, just

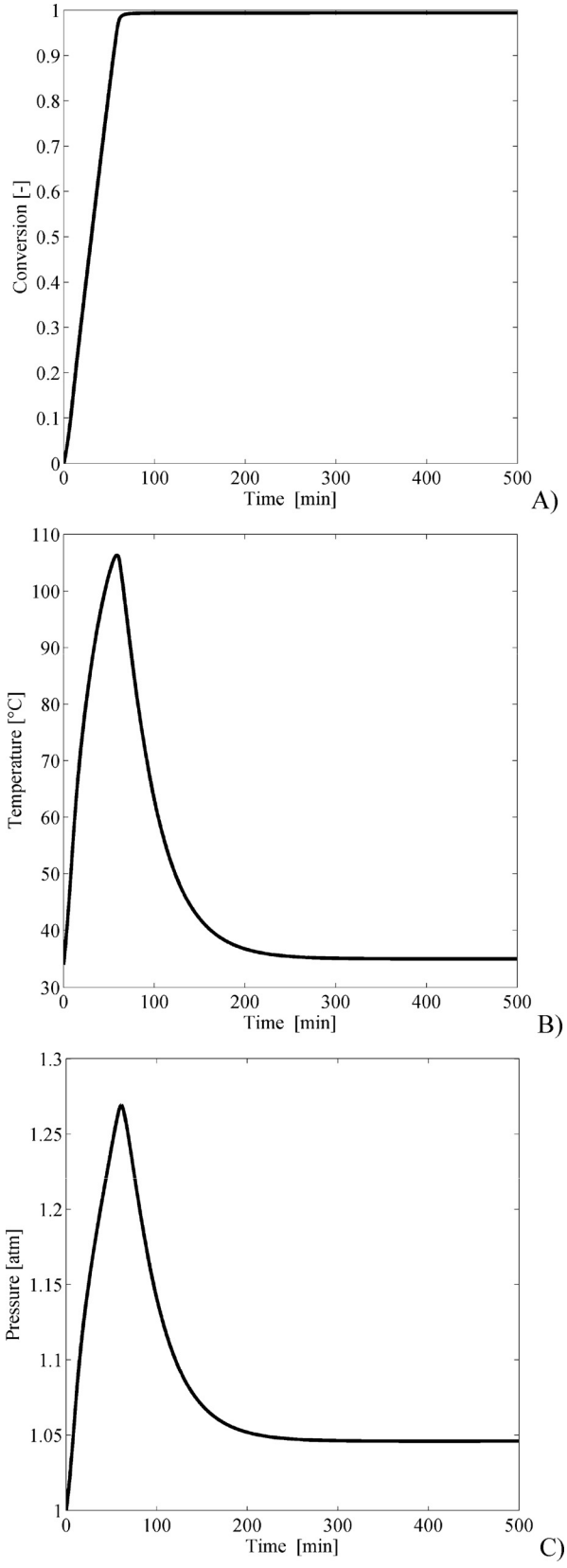

Fig. 3 – (A) Conversion, (B) temperature and (C) pressure vs. time profiles for the nitration of 4-Chlorobenzotrifluoride in mixed acids under normal industrial operating conditions.

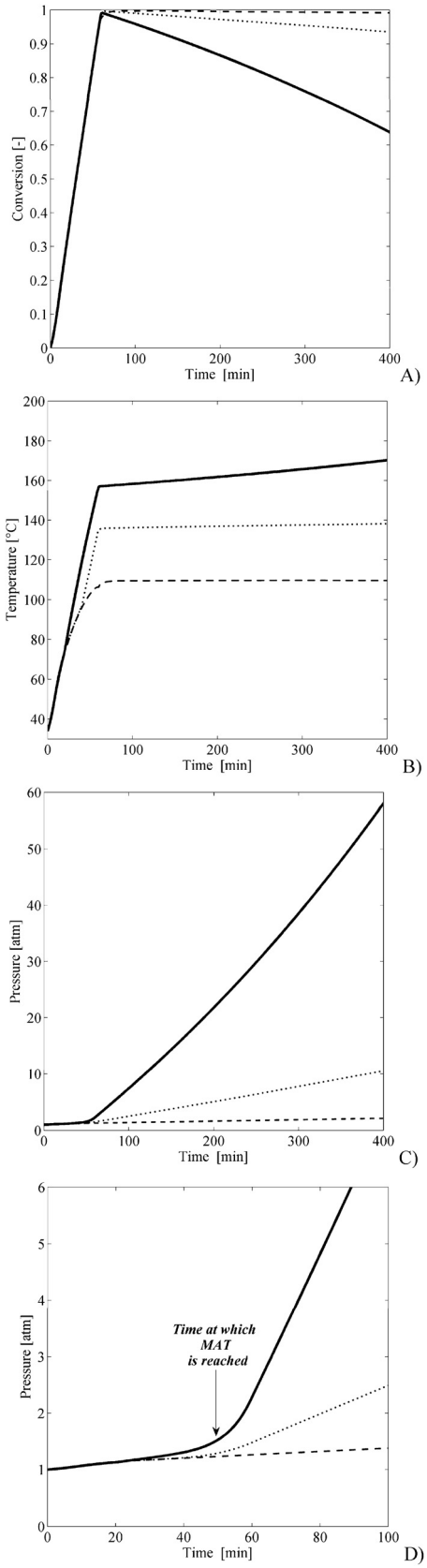

Fig. 4 – Comparison of: (A) Conversion, (B) temperature, (C) pressure and (D) detail of pressure vs. time profiles for the nitration of 4-Chlorobenzotrifluoride in mixed acids under different upset operating conditions. Cooling system failure at: 1/3 (—), 2/3 (· · ·) and 1.5 (- - -) of the dosing period.

before reaching 100%, starts to decrease quite rapidly because of the fast decomposition reaction (at about 400 min, 40% of the desired product C has been decomposed and, therefore, unavoidably lost, see Fig. 4A). The temperature profile (Fig. 4B) does not show peaks (it increases continuously) because the cooling system is broken and, consequently, the reactor is working in practically adiabatic conditions. In particular, it is interesting to observe the slope of the pressure vs. time profile (Fig. 4C). Until 50–55 min, the pressure increases almost linearly according to the reactor temperature increase due to the desired reaction, but, after this time, in correspondence of which the reactor has reached the temperature of 141 °C (that is, the *MAT*), there is a huge trend change: the pressure starts to increase very quickly showing that its increase cannot be related to the temperature increase only. Moreover, starting from 50 to 55 min (that is, about half an hour after cooling system breakdown) also the conversion to the desired product begins to decrease: the decomposition reaction has been triggered with high rates. Observing Fig. 4C, it is possible to see that the maximum pressure that could be reached into the reactor after 400 min is about 60 atm. Such a value is too high to be sustained by common industrial reactors equipped for ambient pressure syntheses. Therefore, in correspondence of a critical pressure the reactor will explode if the emergency relief system cannot handle such an event, releasing into the environment the decomposition gases. Assuming a critical pressure value of about 6 atm, reactor explosion is expected in about 85 min, that is, about 1 h after cooling system breakdown.

If the cooling system failure occurs when the dosing period is almost completed, that is at 2/3 of the dosing period (dotted lines in Fig. 4), the conversion with respect to C increases quite rapidly (the slope is similar to that exhibits by the case of failure at 1/3 of t_{dos}) due to the desired reaction and, then, starts to decrease gently because of the low decomposition of C (at 400 min, about 6.5% of the desired product has been decomposed and, therefore, unavoidably lost, see Fig. 4A, dotted lines). Even in this case, the temperature profile (Fig. 4B, dotted lines) does not show peaks since the cooling system is broken. In particular, it is interesting to observe that the pressure vs. time profile (Fig. 4C, dotted lines) does not exhibit a clear change in its trend: it can be argued that the pressure increase is not linear but the decomposition kinetics is slow enough to avoid clear changes in the pressure vs. time profile. In this case, the critical pressure of 6 atm is reached after about 235 min (against 85 min when the failure occurs at 1/3 of t_{dos}) and the maximum pressure that can be reached is much lower (about 10.6 atm instead of 60 atm). Therefore, this second accidental scenario seems less dangerous than that previously analyzed. It is worth to notice that, even if *MAT* is reached only after 757 min from the starting of the dosing period, the reactor can collapse earlier because of the critical pressure overcome in correspondence of about 235 min.

Finally, if the cooling system failure occurs after the completion of the dosing period, as the sake of example at 1.5 of the dosing period (dashed lines in Fig. 4), the conversion with respect to C increases due to the desired reaction and only a slight decrease can be noticed (at 400 min, about 1% of the desired product has been decomposed, see Fig. 4A). Even in this case, the temperature profile (Fig. 4B) does not show peaks since the cooling system is broken. Observing the pressure vs. time profile (Fig. 4C) it can be noticed that the pressure increase is almost linear because the decomposition kinetics is very slow. The critical value of the pressure is never reached:

Table 4 – Report of the main system variables at both 400 min after the start of the dosing and in correspondence of 6 atm (critical pressure).

Time after the failure (min)	Failure at 1/3 of t_{dos}				Failure at 2/3 of t_{dos}			
	5	10	15	20	5	10	15	20
Pressure after 400 min (atm)	1.3	1.5	2.0	3.2	2.0	3.0	5.4	10.6
Conversion after 400 min (%)	41.6	49.8	57.7	65.3	74.5	82.1	88.8	93.5
Temperature after 400 min (°C)	86.0	96.8	107.0	116.8	106.4	116.5	126.9	138.3
Conversion at $P = 6$ atm (%)	–	–	–	63.2	–	79.9	88.3	96.7
Temperature at $P = 6$ atm (°C)	–	–	–	114.0	–	115.8	126.9	137.1
Time at which 6 atm are reached (min)	–	–	–	1067	–	1054	456	235
Time at which MAT is reached (min)	–	–	–	–	–	–	–	757

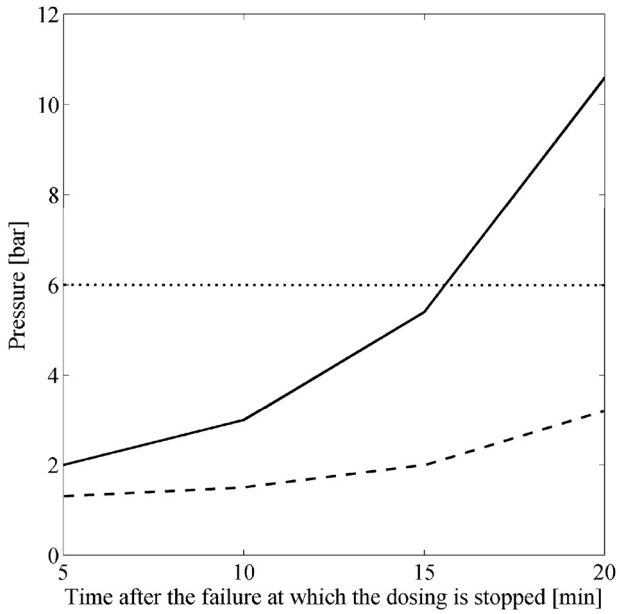

Fig. 5 – Pressure reached into the reactor (after 400 min from the starting of the dosing) as a function of the time after the cooling system failure at which the dosing is stopped. Legend: failure at 1/3 of the dosing time (- - -); failure at 2/3 of the dosing time (—); threshold value of pressure (· · · ·).

this accidental scenario is definitely less hazardous than those previously analyzed.

Therefore, considering the first two accidental scenarios (that is, cooling system failure at 1/3 and 2/3 of t_{dos}), which are the most critical from the safety point of view, it is possible to ask for if an external intervention (as the sake of example, a stop of the dosing pump) can prevent or not the reactor collapse (or the breakage of the rupture disk). Fig. 5 reports the maximum pressure reached into the reactor after 400 min from the starting of the dosing vs. the time at which the dosing is stopped by an operator after the cooling system failure (it is supposed that an alarm drills in the control room when the absence of a coolant flow rate in the jacket is detected). As it can be observed from both Fig. 5 and Table 4 (that reports the main system variables values at both 400 min after the start of the dosing and in correspondence of 6 atm), when the failure occurs at 2/3 of t_{dos}, the reactor can explode (within 235 min) if the dosing is not stopped after a maximum of 16 min from the starting of the cooling system breakdown. If the dosing is stopped after only 5 min later than the failure, the reactor cannot collapse while, when it is stopped within 10 min, the reactor can explode (or the rupture disk can be broken) only after over 17 h. On the contrary, if the failure occurs at about 1/3 of the dosing period, no reactor collapse is expected for over 400 min (see Fig. 5). The *MAT* is reached only in the case of stop of the feeding after 20 min.

From these evidences it is possible to conclude that, if no interventions such as stop of the dosing are done during the accident, when the cooling system failure occurs at 1/3 of the dosing period the situation is much more critical than in the case of failure at 2/3. But, if interventions are undertaken, the case in which the failure occurs at 2/3 of t_{dos} can be more hazardous than the other because the reactor is always expected to collapse (even if in different times) if the dosing is not stopped within 10 min or less.

4. Conclusions

In this work, a detailed simulation of a cooling system failure occurring during the industrial synthesis of 4-Chloro-3-nitrobenzotrifluoride, an intermediate for the production of a well known herbicide, has been carried out and compared with both literature and experimental data obtained through adiabatic calorimetry. Results have shown that, during normal operating conditions, no runaway due to the decomposition of the reacting mixture can occur because the kinetics of this reaction is too low to be thermally appreciated, as indicated also by the ARC results.

On the contrary, during upset operating conditions arising from a cooling system failure taking place before the dosing time completion, a runaway of the desired nitration reaction followed by a decomposition of the reacting mixture is expected, if no interventions (such as stop of the dosing) are undertaken. In the first case investigated (failure at 1/3 of t_{dos}), the *MAT* parameter is largely overcome and a runaway event takes place. In the second case (failure at 2/3 of t_{dos}) even if the *MAT* value is not overcome, due to the slow decomposition reaction the reactor pressurization will take place. No runaway is expected following a cooling system failure after dosing is completed. On the contrary, if some interventions are undertaken, the case in which the failure occurs at 2/3 of t_{dos} can be more hazardous than the others because the reactor is always expected to collapse (even if in different times) if the dosing is not stopped within 10 min or less.

In conclusion, simulating different accidental scenarios that can arise from the same initiating event (in this case-study, the cooling system failure) can lead to a more realistic estimation of the real consequences and frequencies associated to an initiating event, therefore helping in obtaining realistic results from a Quantitative Risk Analysis.

Appendix A.

The following kinetic scheme summarizes the main reactions considered into the 4-Chloro-3-nitrobenzotrifluoride synthesis:

1. Desired nitration $A_{(l)} + B_{(l)} \xrightarrow{k_1} C_{(l)} + D_{(l)}$ (A.1)

2. Decomposition $C_{(l)} \xrightarrow{k_2} G_{(g)}$ (A.2)

where A represents the species 4-Chlorobenzotrifluoride, B is the nitronium ion, C is 4-Chloro-3-nitrobenzotrifluoride (desired product), D is water and G is a gaseous pseudo species originated by the decomposition of the reacting mixture (formally, C).

According to such hypotheses, reaction rates can be expressed as follows:

1. Desired nitration $r_1 = A_1 \cdot \exp\left(-\frac{E_{att,1}}{RT}\right) \cdot [A] \cdot [B]$ (A.3)

2. Decomposition $r_2 = A_2 \cdot \exp\left(-\frac{E_{att,2}}{RT}\right) \cdot [C]^2$ (A.4)

It is possible to notice that the desired reaction (A.3) exhibits a simple kinetic expression of (1, 1) reaction order (Maestri et al., 2009b). This is in agreement with other studies on nitration reactions in which the reaction order with respect to the aromatic species to be nitrated (in this case, A) is always 1 (Lunghi et al., 2002). With respect to the reaction order related to the nitronium ion (which is the electrophilic species) different mechanisms are possible. Anyway, whenever there is a large excess of concentrated sulfuric acid as dehydrating agent (as in this case) the observed reaction order is 1 (but is 2 when other acids, as the acetic acid, are used). Observing the decomposition reaction kinetics (A.4), it is possible to notice that it exhibits a second reaction order with respect to the desired product (species C). Even in this case, this result is in agreement with previous studies on other nitration systems (Lunghi et al., 2002). A possible explanation is that the presence of the mixed acids induces strong instabilities in the final reacting mixture leading to its decomposition following a kinetic law strongly dependent on the concentration of the product C (which contains the nitro group).

The reactive steps during normal operating conditions can be modeled through the following system of ordinary differential equations (ODE), in dimensionless form, expressing (see the Nomenclature section for the meaning of the different symbols): isoperibolic temperature PI control loop (first equation), energy balances on both jacket (second equation) and reactor (third equation), pressure evolution into the reactor (forth equation) mass balances on both the desired product C (fifth equation) and the pseudo species G (sixth equation), global mass balance (seventh equation), mixing rule (equation eight), dosing procedure (ninth equation). In the time range $0 \le \vartheta < 1$:

$$\frac{d\tau_{cool,IN}}{d\vartheta} = -K_{pT} \cdot \left[\frac{d\tau_{cool}}{d\vartheta} - \frac{t_{dos}}{K_{iT}} \cdot (\tau_{set,cool} - \tau_{cool})\right]$$

$$\frac{d\tau_{cool}}{d\vartheta} = \theta_{cool} \cdot (\tau_{cool,IN} - \tau_{cool}) + NTU_{cool} \cdot \upsilon \cdot (\tau - \tau_{cool})$$

$$\rho \cdot \upsilon \cdot \frac{d\tau}{d\vartheta} = \frac{d\upsilon_{dos}}{d\vartheta} \cdot \varepsilon \cdot R_H \cdot (\tau_{dos} - \tau) + \left(\frac{d\zeta_1}{d\vartheta} + \frac{d\zeta_2}{d\vartheta} \cdot \frac{\rho_{dos}}{\varepsilon \cdot \upsilon_{dos}}\right) \cdot \Delta\tau_{ad,1} + \frac{d\zeta_2}{d\vartheta} \cdot \Delta\tau_{ad,2} - St \cdot \upsilon \cdot (\tau - \tau_{cool}) - St_{ext} \cdot (\tau - \tau_{ext})$$

$$\frac{dp}{d\vartheta} = \frac{p}{(\upsilon_{nom} - \upsilon)} \cdot \frac{d\upsilon}{d\vartheta} + \frac{d\zeta_2}{d\vartheta} \cdot n_{B,0} \cdot \frac{R \cdot T_{rif}}{P_{rif} \cdot V_0 \cdot (\upsilon_{nom} - \upsilon)} \cdot \tau + (n_{air} + n_{B,0} \cdot \zeta_2) \cdot \frac{R \cdot T_{rif}}{P_{rif} \cdot V_0 \cdot (\upsilon_{nom} - \upsilon)} \cdot \frac{d\tau}{d\vartheta}$$

$$\frac{d\zeta_1}{d\vartheta} = Da_1 \cdot RE_1 \cdot \kappa_1(\tau) \cdot f_1 - Da_2 \cdot \kappa_2(\tau) \cdot f_2 \quad (A.5)$$

$$\frac{d\zeta_2}{d\vartheta} = Da_2 \cdot \kappa_2(\tau) \cdot f_2$$

$$\frac{d\rho}{d\vartheta} \cdot \upsilon + \rho \cdot \frac{d\upsilon}{d\vartheta} = \varepsilon \cdot \frac{d\upsilon_{dos}}{d\vartheta}$$

$$\frac{d\rho}{d\vartheta} = \frac{\varepsilon \cdot (d\upsilon_{dos}/d\vartheta) \cdot (1 - (1/\rho_{dos}))}{(1 + (\varepsilon/\rho_{dos}) \cdot \upsilon_{dos})^2}$$

$$\frac{d\upsilon_{dos}}{d\vartheta} = 1$$

Initial conditions:

$$\tau_{cool,IN} = \tau_{cool,IN,0}, \quad \tau_{cool} = \tau_{cool,0}, \quad \tau = \tau_0, \quad p = p_0, \quad \zeta_1 = \zeta_2 = 0, \quad \upsilon = \rho = 1, \quad \upsilon_{dos} = 0 \quad (A.6)$$

Some of the equations above changes for $\vartheta \ge 1$ as follows:

$$\frac{d\rho}{d\vartheta} = 0 \quad (A.7)$$

$$\frac{d\upsilon_{dos}}{d\vartheta} = 0 \quad (A.8)$$

Concerning upset operating conditions, it has been arbitrary considered that, at 1/3 (or 2/3 or 1.5) of the dosing period, a cooling system breakdown occurs. In the time range $0 \le \vartheta <$ 1/3 (2/3), the equations are the same as those ones presented for the normal operating conditions case but, for dimensionless times above 1/3 (2/3 or 1.5), the energy balance onto the jacket changes its expression as follows:

$$\frac{d\tau_{cool}}{d\vartheta} = \frac{d\tau}{d\vartheta} \quad (A.9)$$

All other equations keep the same expressions used for the normal operating conditions case. Symbols meaning is reported in the Nomenclature section.

Appendix B.

In order to simulate the thermochemical behavior of a substance subjected to decomposition in an ARC sample holder, only mass and energy balance equations are required.

Considering that, into the system, only a simple decomposition reaction of the desired product C

$$C_{(l)} \Rightarrow G_{(g)} \quad (A.10)$$

takes place with the following microkinetic expression:

$$r_{dec} = k_{dec}(T) \cdot [C]^{\delta} \tag{A.11}$$

As a consequence, the system of ordinary differential equations describing the process in adiabatic conditions is:

$$\begin{cases} \dfrac{d\zeta}{d\vartheta} = Da_{dec} \cdot \kappa_{dec}(\tau) \cdot f_{dec} \\ \dfrac{d\tau}{d\vartheta} = \dfrac{1}{\Phi} \cdot \Delta\tau_{ad,dec} \cdot \dfrac{d\zeta}{d\vartheta} \\ \dfrac{dp}{d\vartheta} = 2.2 \cdot n_{C,0} \cdot \dfrac{d\zeta}{d\vartheta} \cdot \dfrac{R \cdot T_{rif}}{P_{rif} \cdot V_{cielo}} \cdot \tau \\ \qquad + (n_{air} + 2.2 \cdot n_{C,0} \cdot \zeta_2) \cdot \dfrac{R \cdot T_{rif}}{P_{rif} \cdot V_{cielo}} \cdot \dfrac{d\tau}{d\vartheta} \end{cases} \tag{A.12}$$

$$I.C. \quad \vartheta = 0 \Rightarrow \zeta = 0 \quad \tau = \tau_0$$

where $Da_{dec} = k_{dec,rif} \cdot (\hat{\rho}_C / PM_C)^{\delta-1} \cdot t_{rif}$ is the Damkohler number for the decomposition reaction, $f_{dec} = (1 - \zeta)$ conversion function, $\kappa_{dec}(\tau) = \exp(\gamma_{dec}(1 - 1/\tau))$ the dimensionless kinetic constant and Φ the system thermal inertia. Symbols meaning is reported in the Nomenclature section.

References

Alós, M.A., Nomen, R., Sempere, J., Strozzi, F., Zaldívar, J.M., 1998. Generalized criteria for boundary safe conditions in semi-batch processes: simulated analysis and experimental results. Chem. Eng. Process. 37, 405–421.

Balakotaiah, V., Kodra, D., Nguyen, D., 1995. Runaway limits for homogeneous and catalytic reactors. Chem. Eng. Sci. 50, 1149–1171.

Balchan, A.S., Paquet Jr., D.A., Klein, J.A., 1999. Emergency relief adequacy for acrylic polymerization processes. Process Saf. Prog. 18, 71–77.

Bosch, J., Strozzi, F., Lister, D.G., Maschio, G., Zaldívar, J.M., 2004. Sensitivity analysis in polymerization reactions using the divergence criterion. Process Saf. Environ. 81, 18–25.

Casson, V., Lister, D.G., Milazzo, M.F., Maschio, G., 2012. Comparison of criteria for prediction of runaway reactions in the sulphuric acid catalyzed esterification of acetic anhydride and methanol. J. Loss Prevent. Proc. 25, 209–217.

Copelli, S., Derudi, M., Rota, R., 2011a. Topological criterion to safely optimize hazardous chemical processes involving arbitrary kinetic schemes. Ind. Eng. Chem. Res. 50, 1588–1598.

Copelli, S., Derudi, M., Sempere, J., Serra, E., Lunghi, A., Pasturenzi, C., Rota, R., 2011b. Emulsion polymerization of vinyl acetate: safe optimization of a hazardous complex process. J. Hazard. Mater. 192, 8–17.

CSB, 2013. Video Room of Industrial Chemical Accidents, available at: http://www.csb.gov/videoroom (accessed 26.03.13).

Farquharson, J., McNutt, S., Paula, H., Roberts, M., 1997. QRA of chemical reaction systems: the state of the practice. Process Saf. Prog. 16, 219–224.

Gygax, R., 1988. Chemical reaction engineering for safety. Chem. Eng. Sci. 43, 1759–1771.

Jiang, J., Jiang, J.c., Pan, Y., Wang, R., Tang, P., 2011. Investigation on thermal runaway in batch reactors by parametric sensitivity analysis. Chem. Eng. Technol. 34, 1521–1528.

Kidama, K., Hurme, M., 2013. Analysis of equipment failures as contributors to chemical process accidents. Process Saf. Environ. 91, 61–78.

Kossoy, A.A., Akhmetshin, Y.G., 2012. Simulation-based approach to design of inherently safer processes. Process Saf. Environ. 90, 349–356.

Linga, H.L., Wilkins, B.W., van Wingerden, K., 2013. Large-scale Runaway Reaction Tests, available at: www2.gexcon.com/download/cheers.pdf (accessed 26.03.13).

Lunghi, A., Alós, M.A., Gigante, L., Feixas, J., Sironi, E., Feliu, J.A., Cardillo, P., 2002. Identification of the decomposition products in an industrial nitration process under thermal runaway conditions. Org. Process Res. Dev. 6, 926–932.

Luyben, W.L., 2012. Use of dynamic simulation for reactor safety analysis. Comput. Chem. Eng. 40, 97–109.

Maestri, F., Copelli, S., Rota, R., Gigante, L., Lunghi, A., Cardillo, P., 2009a. Simple procedure for optimally scaling-up fine chemical processes. I: Practical tools. Ind. Eng. Chem. Res. 48, 1307–1315.

Maestri, F., Copelli, S., Rota, R., Gigante, L., Lunghi, A., Cardillo, P., 2009b. Simple procedure for optimal scale-up of fine chemical processes. II: Nitration of 4-chlorobenzotrifluoride. Ind. Eng. Chem. Res. 48, 1316–1324.

Maria, G., Stefan, D.N., 2011. Evaluation of critical operating conditions for a semi-batch reactor by complementary use of sensitivity and divergence criteria. Chem. Biochem. Eng. Q. 25, 9–25.

Mas, E., Bosch, C.M., Recasens, F., Velo, E., 2006. Safe operation of stirred-tank semibatch reactors subject to risk of thermal hazard. AIChE J. 52, 3570–3582.

Pasturenzi, C., Dellavedova, M., Gigante, L., Lunghi, A., Canavese, M., Cattaneo, C.S., Copelli, S., 2013. Thermochemical stability: a comparison between experimental and predicted data. J. Loss Prevent. Proc., http://dx.doi.org/10.1016/j.jlp.2013.03.011.

Roduit, B., Dermaut, W., Lunghi, A., Folly, P., Berger, B., Sarbach, A., 2008. Advanced kinetics-based simulation of time to maximum rate under adiabatic conditions. J. Therm. Anal. Calorim. 93, 163–173.

Shu, C.M., Yang, Y.J., 2002. Using VSP2 to separate catalytic and self-decomposition reactions for hydrogen peroxide in the presence of hydrochloric acid. Thermochim. Acta 392–393, 259–269.

Steensma, M., Westerterp, K.R., 1988. Thermally safe operation of a cooled semi-batch reactor. Slow liquid–liquid reactions. Chem. Eng. Sci. 43, 2125–2132.

Stoessel, F., 1993. What is your thermal risk? Chem. Eng. Prog. 10, 68–75.

Stoessel, F., 2009. Planning protection measures against runaway reactions using criticality classes. Process Saf. Environ. 87, 105–112.

Svandova, Z., Jelemensky, L., Markos, J., Molnár, A., 2005. Steady states analysis and dynamic simulation as a complement in the HAZOP study of chemical reactors. Process Saf. Environ. 83, 463–471.

van Woezik, B.A.A., Westerterp, K.R., 2000. The nitric acid oxidation of 2-octanol. A model reaction for multiple heterogeneous liquid–liquid reactions. Chem. Eng. Process. 39, 521–537.

Varma, A., Morbidelli, M., Wu, H., 2005. Parametric Sensitivity in Chemical Systems. Cambridge University Press, Cambridge.

Zaldívar, J.M., Cano, J., Alós, M.A., Sempere, J.M., Nomen, R., Lister, D., Maschio, G., Obertopp, T., Gilles, E.D., Bosch, J., Strozzi, F., 2003. A general criterion to define runaway limits in chemical reactors. J. Loss Prevent. Proc. 16, 187–200.